Pergamon

Int. J. Solids Structures Vol. 33, No. 10, pp. 1519–1533, 1996

0020–7683/96 $15.00 + .00

0020–7683(95)00103–4

SOME PROBLEMS ABOUT ELASTIC–PLASTIC POST-BUCKLING

ALAIN CIMETIÈRE
ENSMA et Université de Poitiers, Laboratoire de Mécanique Théorique,
40 av. du Recteur Pineau, 86022, Poitiers Cedex, France

and

ALAIN LÉGER
E.D.F.–D.E.R., Mécanique et Modèles Numériques 1, av. du Général De Gaulle 92141,
Clamart Cedex, France

(*Received* 7 *April* 1994; *in revised form* 18 *April* 1995)

Abstract—The first parts of the paper deal with the analysis of simple models of elastic–plastic post-buckling. Attention is drawn to the specific effects, on the one hand, of the elastic–plastic non-linearity, and on the other hand, of the geometrical non-linearity. Both analytical arguments and numerical computations are used, without any asymptotic assumptions. In the next part, the post-buckling of a compressed beam, chosen as an example closer to a real structure than the simple models, is computed by a finite element software. In each case, we get information about the global shape of the solution branches.

As the main qualitative result of all these computations, we observe that the elastic–plastic behavior may lead to monotonous strictly increasing load/displacement curves. By comparison with the non monotonous curves usually deduced from asymptotic calculations, these results then stand for counter examples. Consequently, the paper aims at suggesting a special care when a post-buckling analysis is carried out in order to get maximal loads. The necessity of being careful is related to the kind and the number of problems that are presently open for an elastic–plastic bifurcation theory.

INTRODUCTION

This paper is devoted to some essential qualitative features of the post-buckling of elastic–plastic structures. Concerning the mechanical behavior, several results now belong to the acquired knowledge. They deal for instance either with the criterion of the loss of uniqueness, or with the corresponding bifurcated branches. We will recall these results as far as necessary to understand the purpose. From the engineer's standpoint, the main reason for having a good knowledge of the post-buckling behavior is the calculation of maximal loads. We will try to return to all these aspects, and to discuss finally the global shape of the bifurcated branches, in the light of several direct computations.

So let us recall the main characteristics of elastic–plastic buckling and post-buckling. The first one we want to remember deals with the incipient buckling which involves an eigenvalue problem associated with a velocity problem. The solution of the incipient buckling problem has first been given by Hill (1958, 1959), using the so-called elastic solid comparison method which gives the smallest eigenvalue (presently known as Hill's critical load) and the corresponding buckling mode for a large class of elastic–plastic buckling problems. The first complete result for the existence of different initial velocities was given many years later by Cimetière (1984, 1987). It states that there exist two positive values of the load, say λ_a and λ_b, where λ_a is strictly lower than λ_b and with the following properties:

- the initial velocity problem has only the fundamental solution for any positive λ smaller than λ_a;
- for any λ strictly between λ_a and λ_b, the problem has at least one more solution, transverse to the fundamental one;
- under generic assumptions, it has been established at the same time that λ_a coincides with the tangent modulus critical load given by Hill's criterion, and that λ_b is the

reduced modulus critical load introduced by Engesser (1889) and Von Karman (1910).

The calculations of these critical loads can be found in the work of Katchanov (1975) in the case of beams or simple models. Since we want, in particular, to point to the differences between elasticity and plasticity from the bifurcation standpoint, let us remark that this situation means that plastic buckling involves a continuum of eigenvalues, contrary to the well-known results of Euler buckling of elastic structures.

Up to now, the post-buckling behavior within elastic-plasticity has essentially been studied for simple structures using asymptotic methods and concerns only the branch starting from the lowest eigenvalue. These methods have led to expansions of the form:

$$\lambda = \lambda_c + \lambda_1 \xi + \lambda_2 \xi^{1+\beta} + \ldots, \quad \text{with } \lambda_1 > 0, \lambda_2 < 0, 0 < \beta < 1. \tag{1}$$

The variable ξ is a measure of the buckled deflection, λ_c is Hill's critical load. There is no matter with λ_c, nor with λ_1. Let us recall that λ_1 is strictly positive, that is, the branch is initially strictly increasing even for a symmetric structure, which is a major difference with respect to the elastic case (see for instance Potier-Ferry, 1985). This appears as an elementary consequence of the material properties which lead to a statement of the rate problem in terms of a variational inequality on a convex cone. Consequently the usual bifurcation framework, in which the initial velocity is proportional to the buckling mode, no longer applies.

The next step for which the material properties have a major influence is the nonlinear term of eqn (1). Since several different ways (Hutchinson, 1973a,b, 1974; Léger and Potier-Ferry, 1988, 1993) have been used for its computation, neither the coefficient λ_2 nor the fractional exponent β seem open to discussion. Moreover, a recent work by Camotim and Roorda (1993) has explored the sensitivity of λ_c, λ_1, λ_2 and β with respect to a distribution of residual stresses. For the present purpose, their results can be interpreted as stability or genericity results. From this point of view, they are another proof that there is no matter with these terms.

The specificity of the non-linear term in eqn (1), namely the fractional exponent, clearly appears as a consequence of the growth of an unloading zone in the structure. This growth means that the domain of strict loading, that is, the domain in which the behavior can be described by an equation, is a domain which varies as the structure undergoes post-buckling. This variation introduces a free boundary into the bifurcation problem and is the cause of the fact that neither the classical methods of post-buckling analysis (Lyapunov–Schmidt for example) nor the general results on the behavior of the bifurcated branches (for example Rabinowitz, 1973) still hold. Moreover, since λ_2 is negative, the question of whether we get a maximal load or not is certainly a real question.

In such a situation, no result exists, as far as the present writers are aware, concerning the existence of the branches for a continuous medium (let us recall that the aforementioned results by Hill or Cimetière only deal with the initial velocities), their regularity and, contrary to the Rabinowitz (1973) results, their behavior far from the buckling point. As a consequence of this lack of general results, we don't know anything in particular about the missing terms in expansion (1). Consequently, this expansion is used for the computation of the maximal loads after a truncation beyond the term of exponent $1+\beta$. But it is worth seeing for example that this maximal load could change a lot, depending on whether the first missing term in eqn (1) has a big coefficient or not with respect to λ_2, or has an exponent close to $1+\beta$ or not.

In fact, two kinds of more complete results exist for a simple model. On the one hand an expression of the first following term has been given by Hutchinson (1973a), but these missing terms have never been given for any more general structure. On the other hand, existence and analycity have recently been studied by Cimetiere *et al.* (1994) in the case of the same model as the one used by Hutchinson. These first results strongly justify the following computations.

In the first part of the present paper, we describe a simple elastic–plastic buckling model, for which we give an explicit computation. The next section deals with another simple model. The difference from the previous model is that it aims to show the effects of the geometrical non-linearities in addition to the constitutive law, which means that we will briefly discuss the different possible choices concerning these non-linearities. As in the first section, a computation of the bifurcated branch starting from the lowest critical load is done by a direct numerical procedure. In the last section, we give the results of the computation, done with a bidimensional elastic–plastic finite element software, of a slightly geometrically imperfect compressed beam. Several comments on all these numerical results will indicate the problems that appear by comparison with what is given by asymptotic theories.

This work only uses very elementary mathematical tools, but is based upon the acquired knowledge about plastic buckling and post-buckling. For instance, we know, for the two degrees of freedom system that will be described in the next section, that the first bifurcation point coincides with the occurence of a neutrally loaded point at an extremal point of the structure, while an unloading zone spreads out from this point on the corresponding branch. Such a knowledge, of course, will be a guide for the computations.

A SIMPLE MODEL

This section relates in detail the different steps of the computation of the bifurcated equilibria of a simple model. This model is from Hutchinson (1973a), and is recalled here from the standpoint of a direct computation without any asymptotic assumptions, when the previous analyses essentially used asymptotic methods, at least up to the authors' knowledge. As represented in Fig. 1, this model is made of two rigid bars, rigidly connected to each other with a right angle at the middle of the horizontal one, the whole structure being supported by a continuous distribution of elastic–plastic vertical springs. Since this model will be used only for linearized strains, no more geometrical description is required. The structure is loaded by a vertical force λ at the top of the vertical bar whose length is L. The horizontal bar has a length 2, from -1 to $+1$ on the horizontal axis x. Because of the rigidity of the structure, this model has only two degrees of freedom, namely the vertical displacement u and the rotation θ, so that the quantity

$$\varepsilon(x, \lambda) = u(\lambda) + x\theta(\lambda) \tag{2}$$

represents the deformation of the spring at the position x.

This model is well known as a good one for understanding the main qualitative features of plastic post-buckling since it is the simplest model that allows an analysis of the growth of the unloading zone. Actually, the model of Shanley (1947), from which the present

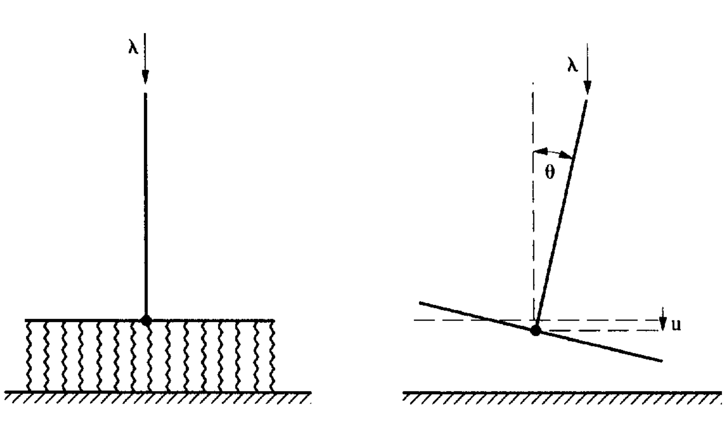

Fig. 1. J. W. Hutchinson's simple model.

model is derived, can give information about the buckling point, but cannot give anything about the post-buckling if it is applied to the behavior of a continuous medium.

In fact, the model is a bit simpler than Hutchinson's original one, since we have omitted the non-linear elastic horizontal spring, connecting the rigid wall to the top of the vertical bar, and which was inserted into the mechanism to take into account the geometrical non-linearities. The kinematics is then fully linearized, and the non-linearity is due to the material properties only. The effect of non-linear kinematics in addition to elastic-plasticity will be discussed in the next section.

The equilibrium problem for this structure then reads as follows:

$$\left.\begin{aligned} \lambda &= \int_{-1}^{+1} \sigma(x)\,\mathrm{d}x \\ \lambda L\theta &= \int_{-1}^{+1} x\sigma(x)\,\mathrm{d}x \end{aligned}\right\} \tag{3}$$

where $\sigma(x)$ classically denotes the stress, that is the compressive force in the spring at the position x.

A classical incremental elastic–plastic constitutive law is chosen for the behavior of the springs. This means that the stress and the strain velocities are related in the following way:

$$\dot{\sigma} = E_{\mathrm{T}}\dot{\varepsilon}(x), \text{for plastic loading} \tag{4a}$$

$$\dot{\sigma} = E\dot{\varepsilon}(x), \text{for elastic loading, or for unloading.} \tag{4b}$$

E and E_{T} are the Young modulus and the tangent modulus of a bilinear traction curve which is the same for all the springs, and the dot stands for a derivative with respect to a time-like parameter.

The configuration of the structure is assumed to be such that no buckling occurs in the whole elastic range, which means that the equilibrium problem has only the trivial solution of uniform compression up to the limit of elasticity. Consequently, the relation (4a) holds everywhere in $[-1, +1]$ before bifurcation occurs. Then, a result, known as the Shanley criterion, asserts that the loss of uniqueness happens together with a neutrally loaded point at one end of the structure (-1 or $+1$ depending on the sign of the initial velocity $\dot{\theta}$ of the buckled solution; see for instance Hutchinson (1973a) for more details). Let us choose for instance the case of a positive deflection θ. Then, beyond the bifurcation point, the corresponding branch actually involves a boundary $X(\lambda)$ in $[-1, +1]$, such that (4b) holds in $[-1, X(\lambda)]$ and (4a) holds in $[X(\lambda), +1]$. Moreover, the kinematics imply the following continuity relation for the position of the boundary $X(\lambda)$:

$$\dot{\varepsilon}(X(\lambda)) = \dot{u} + X(\lambda)\dot{\theta} = 0. \tag{4c}$$

Since the constitutive law (4) involves velocity relations, the equilibrium equations must be changed into the incremental form:

$$\left.\begin{aligned} \dot{\lambda} &= \int_{-1}^{+1} \dot{\sigma}\,\mathrm{d}x \\ \dot{\lambda} L\theta + \lambda L\dot{\theta} &= \int_{-1}^{+1} x\dot{\sigma}(x)\,\mathrm{d}x \end{aligned}\right\}. \tag{5}$$

Remark 1.

Hill's sufficient uniqueness condition naturally applies well for this two-degrees of freedom-model, and we easily get that the solution of uniform compression is unique as long as the load is lower than $\lambda_c = 2E_T/3L$. Moreover, it is known that a slightly more complicated model is required for the occurrence of a tangent bifurcation at λ_c (Triantafyllidis, 1983). Then the bifurcation is actually transverse for the model at hand, and the analysis will deal with the corresponding branch.

Thanks to the above-mentioned description of the bifurcated solutions, eqns (4) and (5) can be rewritten as:

$$\left.\begin{aligned} \dot{\lambda} &= \int_{-1}^{X(\lambda)} E(\dot{u}+x\dot{\theta})\,\mathrm{d}x + \int_{X(\lambda)}^{+1} E_T(\dot{u}+x\dot{\theta})\,\mathrm{d}x \\ \dot{\lambda}L\theta+\lambda L\dot{\theta} &= \int_{-1}^{X(\lambda)} E(\dot{u}+x\dot{\theta})x\,\mathrm{d}x + \int_{X(\lambda)}^{+1} E_T(\dot{u}+x\dot{\theta})x\,\mathrm{d}x \\ \dot{u}+X(\lambda)\dot{\theta} &= 0 \end{aligned}\right\} \tag{6}$$

where the main unknown is the free boundary $X(\lambda)$. We will omit the explicit dependance on λ in the remainder.

The integrations can be done very simply with respect to x in eqn (6) which finally leads to the following system:

$$\left.\begin{aligned} \dot{\lambda} &= [-\tfrac{1}{2}(E-E_T)-(E+E_T)X-\tfrac{1}{2}(E-E_T)X^2]\dot{\theta} \\ \dot{\lambda}L\theta &= [\tfrac{1}{3}(E+E_T)+\tfrac{1}{2}(E-E_T)X-\tfrac{1}{6}(E-E_T)X^3-L\lambda]\dot{\theta} \end{aligned}\right\}. \tag{7}$$

In order to simplify the notations, let us denote by α and β the following material parameters:

$$\alpha = \frac{E+E_T}{E-E_T}, \quad \beta = E-E_T, \tag{8}$$

and define two functions f and g of the position X of the boundary:

$$\left.\begin{aligned} f(X) &\underset{\text{def}}{\equiv} -\tfrac{1}{2}X^2-\alpha X-\tfrac{1}{2} \\ g(X) &\underset{\text{def}}{\equiv} -\tfrac{1}{6}X^3+\tfrac{1}{2}X+\frac{\alpha}{3} \end{aligned}\right\}. \tag{9}$$

Consequently, system (7) turns to be:

$$\dot{\lambda} = \beta f(X)\dot{\theta}, \tag{10a}$$

$$\dot{\lambda}L\theta = (\beta g(X)-L\lambda)\dot{\theta}. \tag{10b}$$

Remarks 2

- The function $f(X)$ is nullified only once in $[-1, +1]$, precisely at the point $X_1 = -(1-\sqrt{E_T/E})/(1+\sqrt{E_T/E})$. Moreover, $f(X)$ is strictly positive and decreasing in $[-1, X_1]$.
- The function $g(X)$ is positive and increasing in $[-1, +1]$.

Remark 3

The zero X_1 of $f(X)$ is precisely the position of the neutral loading boundary given by Katchanov (1975) when computing the buckling under constant loading. For a beam with a rectangular cross-section, this position of the boundary leads to the so-called critical load of the reduced modulus λ_R.

As simple consequences of these remarks, the following results are easily obtained for the behavior of the bifurcated branch starting from λ_c.

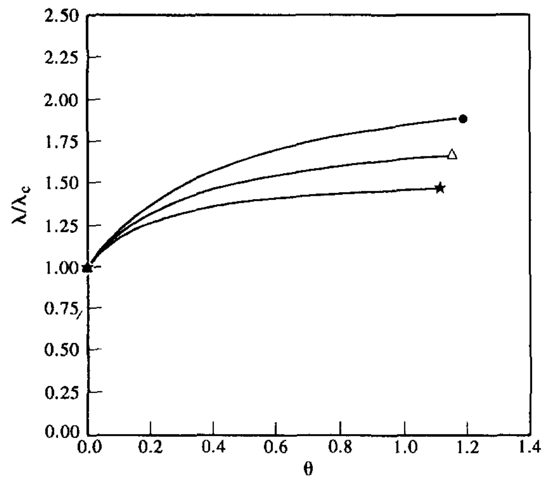

Fig. 2. The load/displacement curve of the simple model (●: $E_T/E = 0.1$, △: $E_T/E = 0.2$, ★: $E_T/E = 0.3$).

Result 1

The ratio $\dot{\lambda}/\dot{\theta}$, that is the slope of the load/displacement curve, tends to zero as $X \to X_1$. Moreover, if $\dot{\lambda}$ is strictly positive, then $\dot{X}$ is strictly positive.

Result 2

For any λ belonging to $[\lambda_c, \lambda_R]$, there exists a boundary $X(\lambda)$, which is a monotonically increasing function of the load, such that $X(\lambda) \to X_1$ as $\lambda \to \lambda_R$.

Remark 4

All the preceeding results do not depend on E_T/E, of course within the limits $0 < E_T/E < 1$.

A numerical computation of the branch gives a more precise understanding of these results. Assume the dot directly indicates a derivative with respect to the load, and use Remark 2 and Result 2. Then system (10a,b) can be rewritten as:

$$\left.\begin{aligned} \dot{\theta} &= \frac{1}{\beta f(X)} \\ \theta &= \frac{g(X)}{Lf(X)} - \frac{\lambda}{\beta f(X)} \end{aligned}\right\} \qquad (11)$$

which suggests a very simple path following method. Using a small enough ΔX as the control increment, and starting from $X_0 = -1$, $\theta_0 = 0$, $\lambda_0 = \lambda_c$, we get the load/displacement curves plotted in Fig. 2, for $L = 1$ and different values of E_T/E.

According to the qualitative results just given above, the bifurcated branches obtained from the numerical computation of this simple model are monotonous, strictly increasing even for strains much greater than what is usually concerned by the geometrical linearization. It is then interesting to compare these branches with those given by the truncation of expansion (1) explicitly given previously in that case (Hutchinson, 1973a; Léger and Potier-Ferry, 1988). This comparison is plotted in Fig. 3.

Let us notice, from Fig. 3(a), that the comparison shows, simultaneously, the sharp divergence of the two estimates of the solution under increasing deflection, and the correctness of the first terms of expansion (1). Before drawing some more complete conclusions from this computation, the next section will look at the effects of non-linear kinematics.

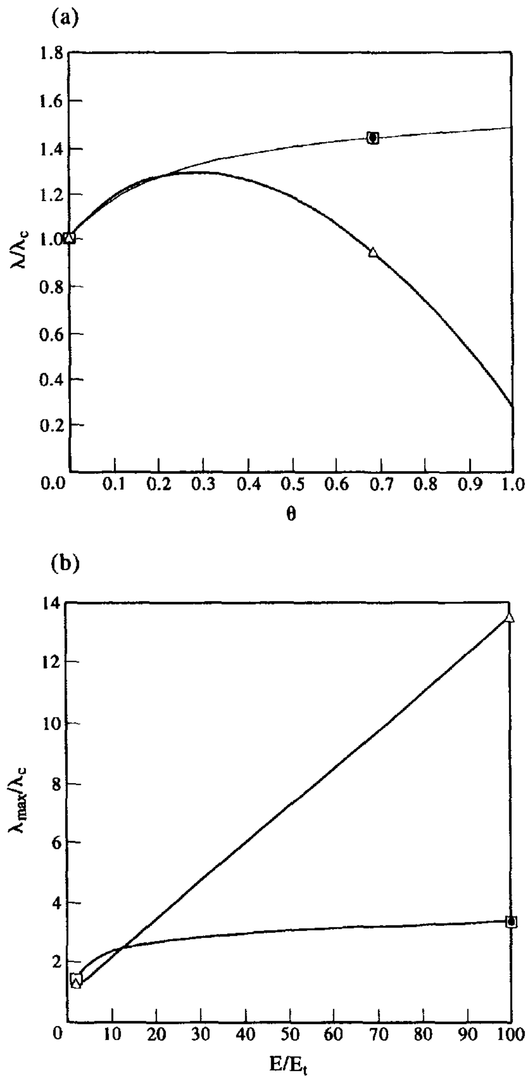

Fig. 3. Comparison between the estimate of the maximal load given by the truncation of the asymptotic expansion and by the direct computation. (a) Load/displacement curve for $E_T/E = 0.3$; (b) maximal load as a function of E/E_T; △ : asymptotic result, ▣ : direct computation.

A GEOMETRICALLY NON-LINEAR MODEL

As in the previous section, we aim at giving the post-buckled branch of a simple model which could be looked at as a first approach of the behavior of a real elastic–plastic structure. Since we want to get a wide enough degree of generality, we know that it is necessary to specify the type of the non-linearities. For a bifurcation analysis, an elastic–plastic structure generically involves two different types of non-linearities. The first one, general to any buckling problem, is related to the large displacements, or even large strains. The second one is specific to elastic–plastic behavior, and essentially accounts for the fact that elastic bifurcation analyses do not hold. Let us recall that Hutchinson's model took these two non-linearities into account, the geometrical one being represented by the horizontal non-linear elastic spring. Moreover it has been established that both are necessary for a convenient buckling analysis of elastic–plastic structures (Cimetière, 1987).

Then we add to the previous model a geometrical non-linearity that we describe below. The model is represented in Fig. 4. Since it will be technically feasible, it is quite justified to look at its post-buckling, and we will study a more classical continuous model in the last section.

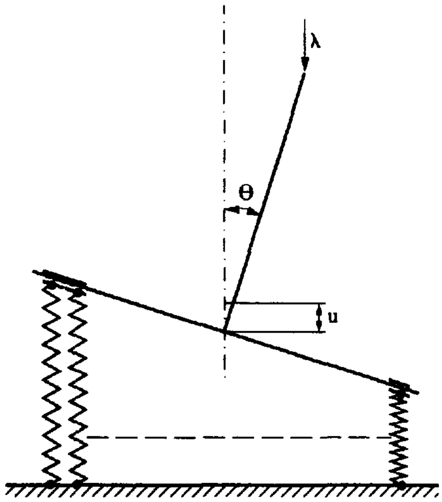

Fig. 4. The first model with non-linear kinematics.

This model is in fact quite similar to the simpler one. The structure is made of two rigid bars, rigidly connected with a right angle, and supported by a continuous distribution of elastic–plastic springs. Since this model is supposed to describe greater strains than the previous one, it is necessary to add some information concerning the springs. At first, they are tied at their bottom, at fixed points of the horizontal axis uniformly distributed on the interval $[-1, +1]$. Secondly, they are constrained, by a guide without friction, to be extended or compressed only along the vertical direction passing through their connection with the horizontal axis. Thirdly, their connection with the initially horizontal bar is assumed to slide without friction. As a last part of this section, we will discuss shortly the effects of these choices.

Using the same notation as in the previous section, the equilibrium of such a mechanical model is described by the following resultant and momentum equations:

$$\left.\begin{aligned} \lambda &= \int_{-1}^{+1} \sigma(x)\,\mathrm{d}x \\ \lambda L \sin\theta &= \int_{-1}^{+1} \frac{\sigma(x)}{\cos^2\theta} x\,\mathrm{d}x \end{aligned}\right\} \tag{12}$$

and the nonlinear strain is now:

$$\varepsilon(x) = u + x\tan\theta. \tag{13}$$

The velocity equations turn out to be:

$$\left.\begin{aligned} \dot{\lambda} &= \int_{-1}^{+1} \dot{\sigma}\,\mathrm{d}x \\ \dot{\lambda} L \sin\theta + \lambda L \cos\theta\dot{\theta} &= \int_{-1}^{+1} \frac{x\dot{\sigma}}{\cos^2\theta}\mathrm{d}x + \int_{-1}^{+1} \frac{2\sin\theta\dot{\theta}}{\cos^3\theta} x\sigma\,\mathrm{d}x \end{aligned}\right\}. \tag{14}$$

The second equation can be changed by observing that the last integral is in fact given by the initial equilibrium equations (12), and the velocity problem is then:

$$\left.\begin{aligned}
&\dot{\lambda} = \int_{-1}^{+1} \dot{\sigma}\,\mathrm{d}x \\
&\dot{\lambda} L \sin\theta + \lambda L \cos\theta\dot{\theta} = \int_{-1}^{+1} \frac{x\dot{\sigma}}{\cos^2\theta}\mathrm{d}x + 2\,\mathrm{tg}\,\theta\lambda L \sin\theta\dot{\theta} \\
&\dot{u} + \frac{X}{\cos^2\theta}\dot{\theta} = 0
\end{aligned}\right\} \tag{15}$$

with the same constitutive relations as for the geometrically linear case.

After the same computations as for the previous model, and using notations (8) and (9), the velocity problem (15) turns into system (16) instead of (10).

$$\left.\begin{aligned}
&\dot{\lambda} = \beta f(X)\frac{1}{\cos^2\theta}\dot{\theta} \\
&\dot{\lambda} L \sin\theta = \beta\left[g(X)\frac{1}{\cos^4\theta} + \frac{\lambda L}{\beta}\frac{(2\sin^2\theta - \cos^2\theta)}{\cos\theta}\right]\dot{\theta}
\end{aligned}\right\} \tag{16}$$

Some of the qualitative features of the previous case persist with the present non-linear kinematics. For instance, the function $f(X)$ reaches zero at the same value X_1 as in the geometrically linear case. Moreover, the slope $\dot{\lambda}/\dot{\theta}$ is still strictly positive in $[-1, X_1]$.

The numerical analysis remains very simple: let us choose the angle θ as the path following parameter. At the step number i, system (16) can be written as:

$$\Delta\lambda_i = \beta f(X_i)\frac{1}{\cos^2\theta_i}\Delta\theta_i \tag{17a}$$

$$\Delta\lambda_i L \sin\theta_i = \beta\left[g(X_i)\frac{1}{\cos^4\theta_i} + \frac{(\lambda_{i-1} + \Delta\lambda_i)L}{\beta}\frac{(2\sin^2\theta_i - \cos^2\theta_i)}{\cos\theta_i}\right]\Delta\theta_i. \tag{17b}$$

Recalling eqn (9), it is readily seen that eqns (17a,b) lead to a polynomial equation, whose coefficients depend on the angle, for the position X_i of the boundary:

$$\begin{aligned}
&-\frac{1}{\cos^2\theta_i}\frac{1}{6}X_i^3 + L\left(\sin\theta_i - \frac{(2\sin^2\theta_i - \cos^2\theta_i)}{\cos\theta_i}\Delta\theta_i\right)X_i^2 \\
&\qquad + \left(\frac{1}{2}\frac{1}{cos^2\theta_i} + \alpha L\left(\sin\theta_i - \frac{(2\sin^2\theta_i - \cos^2\theta_i)}{\cos\theta_i}\Delta\theta_i\right)\right)X_i \\
&+\frac{\alpha}{3\,cos^2\theta_i} + \frac{L}{2}\left(\sin\theta_i - \frac{(2\sin^2\theta_i - \cos^2\theta_i)}{\cos\theta_i}\Delta\theta_i\right) + \lambda_{i-1}\frac{L}{\beta}(2\sin^2\theta_i - \cos^2\theta_i)\cos\theta_i = 0.
\end{aligned} \tag{18}$$

Then solving the free boundary problem turns into finding at each step, the good root of the third degree polynomial equation (18). This is qualitatively interesting because, by the same way as the previous monotonicity result for $X(\lambda)$, this stresses the fact that the global behavior is "governed" by the evolution of the boundary of the unloading zone. The numerical procedure is quite easy and leads to the results plotted in Fig. 5.

The load/displacement curve is actually got as a strictly monotonous curve, which is the main qualitative result for the present purpose. The latter non-linear model will be referred to as Model 2, when the previous one with the linear kinematics will be referred to as Model 1. Both lead to monotonous strictly increasing bifurcated branches.

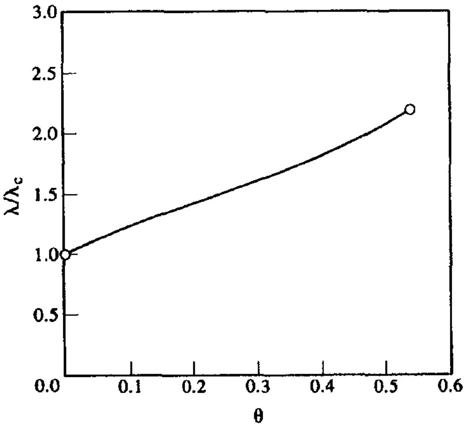

Fig. 5. The load/displacement curve of the simple model with the geometrical non-linearity.

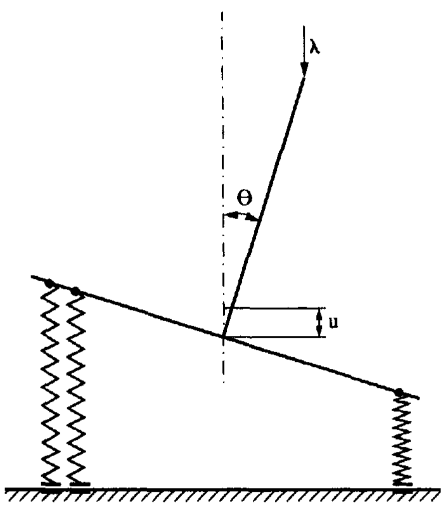

Fig. 6. Another geometrical non-linearity.

Let us, however, observe some differences. The curve plotted in Fig. 5 does not have a decreasing slope as the angle θ is great enough, contrary to the geometrically linear case. In fact, it seems that this appears together with a reloading process in the structure, which means that the boundary $X(\lambda)$ is not a monotonous function of the load, and turns back towards -1. This specificity is probably strongly dependent on the method of modelling the non-linear geometry. This is not that different from Hutchinson's original model where it has been noticed that some conditions are required for the coefficients of the non-linear elastic spring for obtaining an unloading zone. But in the present case, it is probably related to the fact that the geometrical non-linearity is, in some sense, stabilizing. This suggests a short discussion about the respective effects of the behavior and the geometrical non-linearities. This discussion can be carried out, at least for our purpose, thanks to another type of geometrically non-linear model. Let us consequently look at the response of the model represented in Fig. 6, whose geometry can be seen as destabilizing. The latter will be referred to as Model 3.

The equilibrium equations are changed into the following:

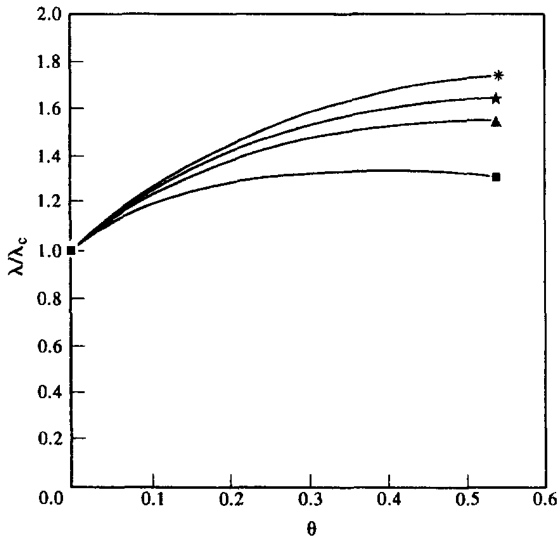

Fig. 7. Load/displacement curves of Model 3 (■ : $E_T/E = 0.3$, ▲ : $E_T/E = 0.1$, ★ : $E_T/E = 0.05$, ✱ : $E_T/E = 0.01$).

$$\left.\begin{aligned} \lambda &= \int_{-1}^{+1} \sigma(x)\,\mathrm{d}x \\ \lambda L \sin\theta &= \int_{-1}^{+1} x\sigma(x)\cos\theta\,\mathrm{d}x \end{aligned}\right\}$$

and the strain is given by $\varepsilon(x) = u + x \sin\theta$.

Then the same analysis and numerical procedure as those of Model 2 lead to the solution branches plotted in Fig. 7.

The qualitative result is now that the first bifurcated branch can be either monotonous strictly increasing, or non monotonous, first increasing then decreasing, depending on the ratio E_T/E. The same kind of phenomena has been described by Needleman and Tvergaard (1976) who observed that the solution branches can be monotonous or non monotonous, depending on the exponent n of a Ramberg–Ogsgood type constitutive relation. This is an interesting consequence of the fact that the problem involves two different non-linearities. In order to have a better interpretation of the cumulative effects of these non-linearities, let us recall the behavior of simple models, geometrically quite similar to previous Models 1, 2 and 3, but with a linearly elastic constitutive law. Elementary calculations lead to the bifurcation diagram represented in Fig. 8.

Qualitative and quantitative analyses of elastic–plastic post-buckling have established that immediate elastic–plastic post-buckling is possible under increasing load, even for a symmetric structure, because the load increment is balanced by a local increase of rigidity (see for instance Léger and Potier-Ferry, 1993). Recalling Figs 2, 5, 7 and 8, this suggests we can guess the following extension:

- if the geometrical non-linearity is such that the elastic bifurcated branch is increasing, then the elastic–plastic branch is strictly increasing;
- if the geometrical non-linearity is such that the elastic bifurcated branch is a constant function, then the elastic–plastic branch is increasing, strictly increasing for any finite deflection;
- if the geometrical non-linearity is such that the elastic-bifurcated branch is decreasing, then the elastic–plastic branch can be either strictly increasing for small values of the tangent modulus, or first increasing then decreasing if the tangent modulus approaches the elastic modulus.

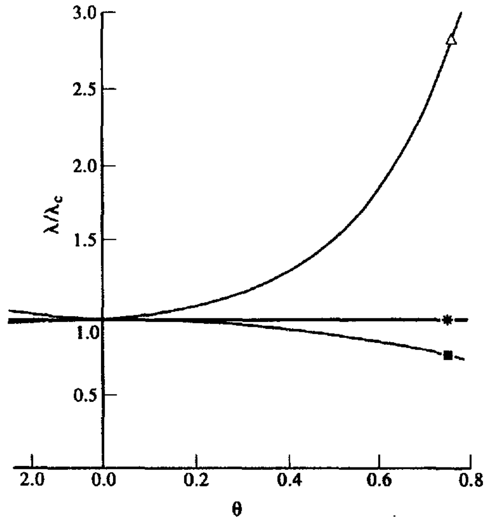

Fig. 8. Post-buckling of the corresponding models in the elastic range. (✱ : Model 1, △ : Model 2, ■ : Model 3).

This can be set as a kind of conjecture, numerically observed in the case of incremental elastic-plasticity: *during immediate post-buckling the material non-linearity always prevails over the geometrical one, contrary to asymptotic behavior which is strongly determined by geometrical non-linearity.*

Anyway, coming back to the main purpose of the present work, we aimed at showing that a strictly increasing bifurcated branch may occur within elastic-plasticity. This is widely proved by these examples.

A STANDARD FINITE ELEMENT COMPUTATION

As a preliminary remark, the authors would like to insist on the fact that this section does not aim at being any kind of proof, even numerical proof, of what is observed with the simple models. At the very most this can be seen as another example. Nevertheless, the method is different, and the model is closer to a real structure than the simpler one. But it is necessary, maybe more than for the previous examples, to give the description of the problem and of the parameters of the computation quite completely, so as to allow the reader to check the results.

The problem at hand is a compressed beam, with clamping boundary conditions at both ends. The computation is done using a bidimensional elastic–plastic finite element software. It is well known that such a computation does not present any fundamental difficulties, but only needs a little care, such as a thin enough mesh size, and very small load increments. Under these natural precautions, it has already been observed (Léger and Potier-Ferry, 1993) that we get convenient buckling deflection and growth of the unloading zone.

The mesh we used has 12×49 elements for the half-beam, which means 2475 nodes for quadratic finite elements. Let l and d be the length of the beam and the width of its cross section respectively. Then the geometry is such that $l/d = 20$, and the imperfection is an initial deflection equal to $d/25$ at the middle of the beam. The imperfection sensitivity within elastic-plasticity is not the purpose of this paper, but it is known (Hutchinson, 1973b) that such an imperfection leads to a global behavior sufficiently close to the one of the perfect structure. The uniaxial traction curve under increasing load is chosen as:

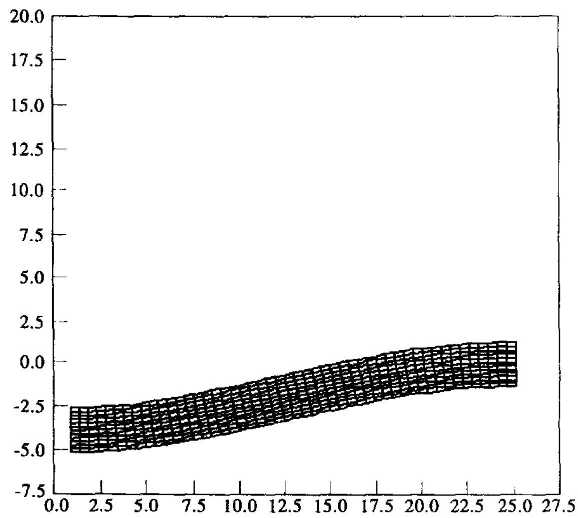

Fig. 9. The buckled shape of the half compressed beam.

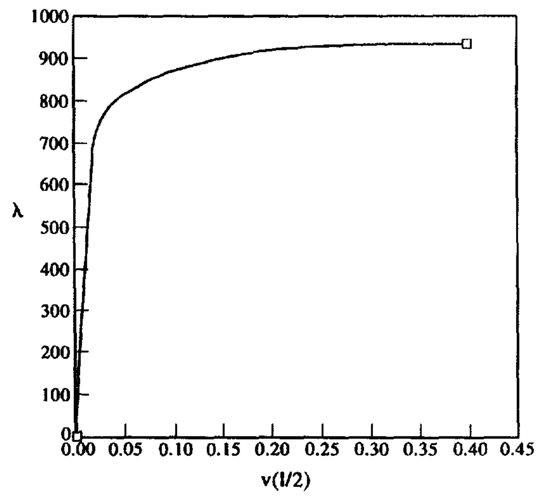

Fig. 10. The load/displacement curve for the compressed beam.

$$\varepsilon = \begin{cases} \dfrac{\sigma}{E}, & \sigma \leqslant \sigma_y \\ \dfrac{\sigma_y}{E}\left[\dfrac{1}{n}\left(\dfrac{\sigma}{\sigma_y}\right)^n - \dfrac{1}{n} + 1\right], & \sigma \geqslant \sigma_y \end{cases} \tag{19}$$

where $n = 10$, $\sigma_y = 305$ MPa, $E = 164864$ MPa.

In addition to this classical form, we have added the usual conditions of incremental plasticity and of isotropic hardening. The Poisson ratio is equal to zero in order to be closer to the usual beam theory. Symmetry boundary conditions are imposed on the cross-section $l/2$, and a longitudinal displacement is prescribed at the end of the beam to modelize both the clamping and the compressive boundary condition.

The non-linear kinematics have been taken into account by actualizing the reference configuration at each step. The solution is plotted in Fig. 9. It represents the deformation of the mesh obtained for one of the last load increments that were computed.

As a specific post-processing, Fig. 10 represents the external compressive load λ corresponding to the imposed axial displacement as a function of the transverse displacement

$v(l/2)$ of the middle fibre at the middle of the beam. The numerical values of the displacement have been normalized by the half thickness of the beam.

COMMENTS AND CONCLUDING REMARKS

As a consequence of all these computations, it is quite clear that a strictly monotonous bifurcated branch may occur within elastic-plasticity. A qualitative reason of this phenomenon is a kind of stabilizing effect of plasticity, because of the onset of an elastic unloading zone. A monotonicity property has been established for the simplest structure (Model 1) using only analytical tools. In the present work, this property has been obtained by an explicit calculation for the first branch. Moreover, results of the same kind have been given in a recent work by Cimetière *et al.* (1994) within the framework of first order ordinary differential equations. This is especially worth seeing since the literature about plastic post-buckling contains many non monotonous curves whose maximal point is known, and used, as the maximal load the structure can support.

In fact, on the one hand, it has been observed that the global shape of the load/displacement curve may depend on the manner of modelling the geometrical non-linearities. On the other hand, it is known that this global shape may change, depending on the material parameters. This was briefly discussed in the present paper.

But this is not the point. Throughout the different computations and results, the paper aimed at suggesting special care where the load/displacement diagram is represented by a non-monotonous curve. As a matter of fact, we have first recalled that an asymptotic result of the type given in eqn (1) does not allow such a representation, even though there is no question about the coefficients and exponents of this expansion. Secondly, we have observed that a direct computation may lead to an increasing curve, either for simple models or for a continuous problem. Moreover, every time a load/displacement curve coming from numerical analysis has been involved as a validation of an asymptotic result, it has, to our knowledge, never been indicated at the same time that the comparison had to be taken carefully since it would not have worked for other values of the parameters.

Since the exact shape of the load/displacement curve for a given structure is usually not known *a priori* before the computation, we state that the asymptotic formula (1) is not a reliable tool for the estimate (even widely approximating) of the maximal load the structure at hand can support. From this point of view, the results given in this paper, either for the simple models or for the compressed beam, must be understood as counter examples.

REFERENCES

Camotim, D. and Roorda, J. (1993). Plastic buckling with residual stresses—1. Postbifurcation behavior. *Dynamics and Stability of Systems* **8,** 219–251.

Cimetière, A. (1984). Flambage naissant des plaques élastoplastiques minces. *C. R. Acad. Sci.* **298,** 99–102.

Cimetière, A. (1987). Sur la modélisation et la flambage des plaques élastoplastiques. Doctoral Thesis, Université de Poitiers.

Cimetière, A., Elkoulani, A. and Léger, A. (1994). Buckling and post-buckling of an elastic–plastic simple model. *C. R. Acad. Sci.* **319,** 1263–1269.

Engesser, F. (1889). Ueber knickfragen. *Schweizerische Bauzeitung* **26,** 24–33.

Hill, R. (1958). A general theory of uniqueness and stability of elastic plastic solids. *J. Mech. Phys. Solids* **6,** 236–249.

Hill, R. (1959). Some basic principles in the mechanics of solids without a natural time. *J. Mech. Phys. Solids* **7,** 209–225.

Hutchinson, J. W. (1973a). Post-bifurcation behavior in the plastic range. *J. Mech. Phys. Solids* **21,** 163–190.

Hutchinson, J. W. (1973b). Imperfection sensitivity in the plastic range. *J. Mech. Phys. Solids* **21,** 191–204.

Hutchinson, J. W. (1974). Plastic buckling. *Adv. Appl. Mech.* **14,** 67–144.

Katchanov, L. (1975). *Eléments de la Théorie de la Plasticité* (French translation). Mir ed, Moscou.

Léger, A. and Potier-Ferry, M. (1988). Plastic post-buckling. *J. Méc. Théo. Appl.* **7,** 819–857.

Léger, A. and Potier-Ferry, M. (1993). Elastic–plastic post-buckling from a heterogeneous state. *J. Mech. Phys. Solids* **41,** 783–807.

Needleman, A. and Tvergaard, V. (1976). An analysis of the imperfection sensitivity of square elastic–plastic plates under axial compression. *Int. J. Solids Structures* **12,** 185–201.

Needleman, A. and Tvergaard V. (1982). Aspects of plastic post-buckling behavior. In *Mechanics of Solids* (Edited by M. J. Sewell and H. G. Hopkins), pp. 453–498. Pergamon Press, Oxford.

Potier-Ferry, M. (1985). Foundations of elastic postbuckling theory. In *Buckling and Post-buckling* (Edited by W. T. Koiter and M. Potier-Ferry), pp. 1–82. Springer, Berlin.

Rabinowitz, P. H. (1973). Some aspects of nonlinear eigenvalue problems. *The Rocky Mountain J. Maths.* **3**, 161–202.

Shanley, F. R. (1947). Inelastic column theory. *J. Aeronaut. Sci.* **14**, 261–267.

Triantafyllidis, N. (1983). On the bifurcation and post-bifurcation analysis of elastic–plastic solids under general prebifurcation conditions. *J. Mech. Phys. Solids* **31**, 499–510.

Von Karman, T. (1910). Untersuchungen über knickfestigkeit mitteilungen über forschungarbeiten. *Ver. Deut. Ing. Forschungsh.* **81.**